Diffusional Surface Voltammetry as a Probe of Adsorption Energetics

ARTICLE *in* ANALYTICAL CHEMISTRY · NOVEMBER 2011

Impact Factor: 5.64 · DOI: 10.1021/ac202564w · Source: PubMed

analytical chemistry

Article

pubs.acs.org/ac

Diffusional Surface Voltammetry as a Probe of Adsorption Energetics

Juan José Calvente,* Miguel Molero, Rafael Andreu, Germán López-Pérez, and Antonio M. Luque

Departamento de Química Física, Facultad de Química, Universidad de Sevilla, 41012 Sevilla, Spain

Supporting Information

ABSTRACT: Direct determination of the adsorption free energy for extremely low surface coverages (Henry limit) requires the use of a technique that must be highly sensitive to both the amount and the energetics of adsorbed molecules. Herein, we demonstrate that *diffusional surface voltammetry* (DSV), which embodies film and stripping voltammetries as two limiting cases, can be used to achieve this goal for electroactive adsorbates. To this end, a general analytical expression for the surface voltammetric peak potential of DSV is derived, which covers the full range of scan rates, bulk concentrations, and adsorptivity of the freely diffusing form of the redox couple, so that the surface redox conversion can be either equilibrated with or transport-isolated from the solution bulk. Strategies to get a quantitative insight into the energetics of electrosorption are outlined, and diagnostic criteria for their application are developed. In particular, it is demonstrated that DSV can be used in its stripping mode to determine group contributions to the adsorption free energy, avoiding possible interferences from intermolecular interactions or formation of oligomeric species. Application of this protocol to the reductive desorption of distinct homologous series of alkylthiolates adsorbed at mercury electrodes has allowed us to determine the contributions of the CH_n groups (n = 0−3) to the free energy of adsorption of these molecules. These estimates are shown to correlate linearly with the corresponding group contributions to the octanol−water partition coefficient, revealing that adsorption of individual hydrocarbon groups at the mercury/solution interface scales with their hydrophobicity. Overall, the present work enlarges the capability of surface voltammetry to probe adsorption energetics down to the micromolar level, and it represents a first step toward the development of a unified treatment of stripping and film voltammetries.

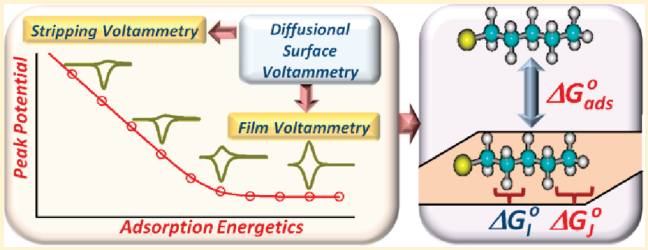

Adsorption/desorption processes at electrified interfaces play a pivotal role in a broad range of fundamental and applied phenomena such as biofilm-based electrochemical processes,[1,2] colloidal stability,[3] cell differentiation,[4] chemical separation,[5,6] and corrosion inhibition.[7,8] In order to uncover the factors that control the adsorption of a target molecule at a given interface, it is important to have an estimate of its free energy of adsorption and, if possible, of its distribution among molecular group contributions. For an electrified interface, this has traditionally been done by fitting theoretical isotherms to electrocapillary and differential capacitance measurements[9,10] and, to a lesser extent, to data obtained by radiochemistry,[11−13] spectrophotometry,[14] and chronocoulometry[15,16] measurements. More recently, advantage has been taken from experimental methods that make use of quartz crystal microbalance,[17,18] second-harmonic generation,[19,20] evanescent wave ring-down spectroscopy,[21] or electrochemically modulated liquid chromatography[22] to derive free energies of adsorption.

White et al.[23,24] have shown that the peak potentials of bulk-equilibrated surface voltammetry can be used to characterize the adsorption energetics of electroactive adsorbates with a strongly adsorbed redox form. This procedure enabled them to determine the methylene group contribution to the adsorption free energy of a series of *n*-alkanethiolates adsorbed at Ag and Hg electrodes.[24,25] To preserve equilibrium with the solution bulk along the voltammetric response, their approach requires the use of rather high adsorbate concentrations (>0.1 mM) and low scan rates (<1 V s^{-1}). However, these restrictions set a limit of ca. one-half monolayer for the minimum amount of adsorbed molecules that can be probed at the peak potential. This is a rather large surface coverage that makes it difficult to avoid some common sources of nonideality, such as interactions between adsorbed molecules or formation of dimeric species, that complicate the estimate of the adsorption free energy. A simple way to overcome this difficulty is to use a stripping voltammetry protocol, which allows for an independent and accurate control of the amount of deposited molecules.[26] This protocol involves the use of low reactant bulk concentrations, within the nanomolar−micromolar concentration range. It includes a preconcentration step to deposit the desired amount of the target adsorbate, and a subsequent voltammetric scan to induce its electrochemical desorption. However, a direct estimate of the adsorption free energy from the peak potential is hampered by the lack of analytical expressions describing the peak potential in terms of the system's parameters. A quantitative description of these stripping voltammograms requires a numerical solution of the relevant mass-transport boundary value problem.[27] In an effort

Received: October 5, 2011
Accepted: November 30, 2011
Published: November 30, 2011

   dx.doi.org/10.1021/ac202564w | *Anal. Chem.* 2012, 84, 1034−1041

to overcome this undesirable situation, we have recently developed a strategy to derive accurate analytical expressions for the stripping voltammetric response of a dilute surface film, under conditions where its redox conversion is controlled by diffusion of the adsorbate.[28] For this particular case, accurate expressions describing the peak potential of a population of either monomeric or dimeric adsorbates were derived in terms of mass-transport and adsorption parameters. However, despite these efforts, a general expression for the peak potential covering the full range of system parameters is still lacking.

From a conceptual viewpoint, the above two approaches can be envisaged as two limiting cases of what can be called *diffusional surface voltammetry* (DSV), in which a redox form is strongly adsorbed and the other is freely diffusing and may display any adsorption strength. Two operational modes can be distinguished in DSV depending on the way the adsorbate deposition is carried out. In the *normal mode*, deposition takes place along the forward scan, which is purposely directed toward potentials that favor adsorption;[29] whereas, in the *stripping mode*, deposition is promoted by poising the electrode during a preset time at the initial potential of the forward scan, that now runs in the desorptive direction.[30] The first mode is the most convenient to preserve equilibrium with the solution bulk and, as stated previously, requires high adsorbate concentrations and low scan rates; whereas the second protocol allows one to probe extremely low surface coverages by employing submillimolar reactant concentrations in the deposition solution.

The present work focuses on a general quantitative description of the DSV peak potential, aimed at covering the full range of scan rates, bulk concentrations, and adsorptivity of the freely diffusing redox form. The derived expression is applicable to both normal and stripping DSV modes, and approaches the solution for *film voltammetry*, whenever the two forms of the redox couple remain strongly adsorbed at the electrode surface. Strategies to determine the adsorption free energy of the reactant, or at least some of its molecular group contributions, are outlined. The feasibility of the present approach is proved by its application to the reductive desorption of distinct homologous series of alkylthiolates adsorbed on mercury electrodes, from which an estimate of the CH_n (n = 0−3) group contribution to the adsorption free energy of these molecules is obtained. As will be shown, these estimates correlate linearly with the corresponding group contributions to the octanol−water partition coefficient, which is commonly taken as an hydrophobicity index. Overall, the present work enlarges the capability of surface voltammetry to probe adsorption energetics down to the micromolar level, and represents a first step toward the development of a unified treatment of stripping and film voltammetries.

RESULTS AND DISCUSSION

Voltammetric Waveshapes for Diffusional Surface Voltammetry (DSV). To illustrate the capability of diffusional surface voltammetry to get insights into the energetics of electrosorption, and bearing in mind its later application to the reductive desorption of alkylthiols, we consider the following redox mechanism:

$$R_{sol} + S_{ads} \overset{K_{aR}}{\rightleftharpoons} R_{ads} + S_{sol}$$

$$R_{ads} \overset{E_s}{\rightleftarrows} O_{ads} + ne^- \qquad (1)$$

where R and O stand for the reduced and oxidized forms of the redox couple, respectively; S represents the solvent, and subscripts sol and ads indicate whether the species is in solution or in the adsorbed state, respectively. K_{aR} is a Langmuir-type adsorption equilibrium constant, E_s is the standard formal potential, and D_R is the diffusion coefficient of reactant R that is used to describe its diffusion toward/from a spherical electrode. The boundary value problem associated with the voltammetric response of reaction 1, together with its numerical resolution for the normal and stripping modes, are described in the Supporting Information. Theoretical voltammograms have been calculated for a typical spherical electrode having a radius of 0.05 cm.

Figure 1 illustrates the voltammetric waveshapes predicted for reaction 1, as a function of bulk concentration of R (c_R^b),

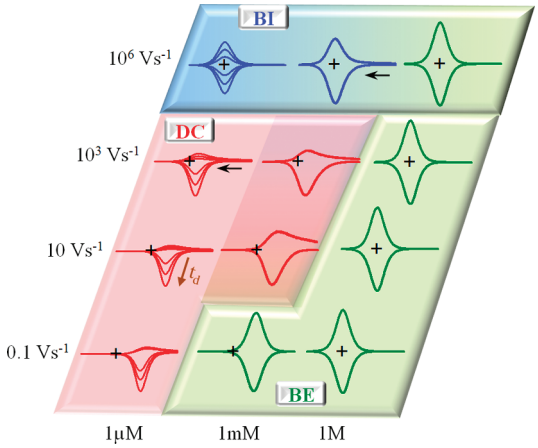

Figure 1. Voltammetric waveshapes for a redox couple whose oxidized form is strongly adsorbed and its reduced form is freely diffusing, as a function of reactant concentration, scan rate, and deposition time (cathodic stripping DSV for reaction 1). Pink, green and blue zones correspond to the limiting cases of a surface redox conversion being controlled by diffusion (DC regime), equilibrated with the solution bulk (BE regime) or isolated from the solution bulk (BI regime), respectively. Crosses help to locate the $E = E_s$ and $i = 0$ coordinates on each voltammogram.

scan rate (v), and deposition time (t_d). For the commonly used scan rates (v < 1000 V s^{-1}), two limiting cases can be distinguished corresponding to low and high enough reactant bulk concentrations, respectively. Below the millimolar level, voltammograms are composed of a cathodic surface wave, having a full width at half-maximum (fwhm) of 75.5/n mV at 25 °C, and a diffusion-type anodic wave. Apart from the evident asymmetry between the cathodic and anodic traces, two additional features of this voltammetric pattern are the dependence of the cathodic peak current on the deposition time and of the cathodic peak potential on the scan rate, which are consistent with an adsorption/desorption process being limited by diffusion of the reduced form of the redox couple. We shall refer to this limiting case as *diffusion-controlled surface redox conversion* (DC regime). On the other hand, above the millimolar level, the voltammetric feature consists of a couple of symmetrical surface waves, having a fwhm of 90.6/n mV at 25 °C, which are independent of the scan rate and deposition time, as expected for a surface redox conversion in the absence of concentration polarization. We shall refer to this limiting case as *bulk-equilibrated surface redox conversion* (BE regime).

dx.doi.org/10.1021/ac202564w | Anal. Chem. 2012, 84, 1034−1041

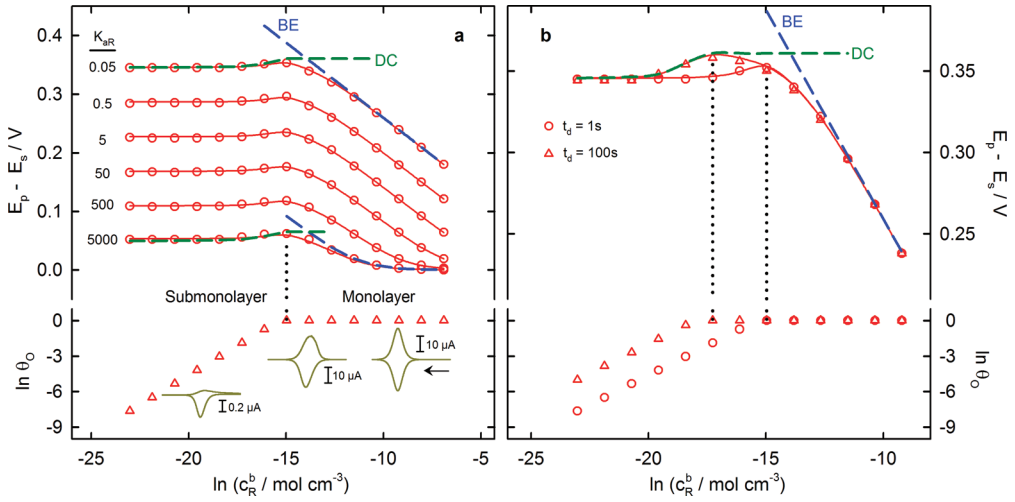

Figure 2. Dependence of the cathodic peak potential (upper panels) and of the logarithm of the surface coverage of the oxidized species (lower panels) on the logarithm of the reactant bulk concentration for the indicated values of (a) the adsorption equilibrium constant (K_{aR}) and (b) the deposition time (t_d). Symbols represent the values obtained from simulated cathodic stripping voltammograms for reaction 1, whereas lines represent the predictions of eq 2 (green dashed lines, DC regime), eq 5 (blue dashed lines, BE regime) and eq 6 (red solid lines). Vertical dotted lines indicate the transition from submonolayer to monolayer surface coverage. Parameter values: $D_R = 8 \times 10^{-6}$ cm^2 s^{-1}, $\Gamma_R^{max} = \Gamma_O^{max} = \Gamma_S^{max} = 8 \times 10^{-10}$ mol cm^{-2}, $c_S^b = 55.5$ M, $r_0 = 0.05$ cm, $\nu = 1$ V s^{-1}, $T = 298$ K, and (a) $t_d = 1$ s and (b) $K_{aR} = 0.05$. Insets (from left to right) represent the voltammetric waveshapes predicted for reactant bulk concentrations 10 μM, 1 mM, and 0.1 M.

Transition between these two limiting cases occurs between the micromolar and millimolar concentration levels at low scan rates, and it shifts toward higher concentrations as the scan rate increases.

A third limiting case is achieved at sufficiently high scan rates (typically >10^4 V s^{-1}), where the time scale of the potential scan is so short that diffusion of R along the cathodic scan is negligible. In this case, the voltammetric wave is centered at the standard formal potential E_s, and its height is dependent on the deposition time, as long as less than one adsorbate monolayer covers the electrode surface. Since this situation corresponds to that of a surface redox conversion isolated from the bulk of the solution, we shall refer to this limiting case as *bulk-isolated surface redox conversion* (BI regime).

As shown in the next section, quantitative criteria to discriminate between the above three limiting cases can be developed from the dependence of the peak potential on both scan rate and reactant bulk concentration. To this end, an analytical expression for the cathodic peak potential, in terms of the relevant parameters of the system, is derived for the case of linear diffusion, which is shown to be a good approximation for the commonly used spherical electrodes, whenever the radius is $r_0 \gg (RTD_R/(nF\nu)^{1/2})$.

Analytical Expressions for the Surface Voltammetric Peak Potential. Figure 2 illustrates how the cathodic peak potential E_p varies with the reactant bulk concentration for distinct values of the reactant adsorption equilibrium constant K_{aR}, whereas Figure 3 depicts its dependence on the scan rate for distinct values of the reactant bulk concentration. At sufficiently low reactant concentrations and intermediate scan rates, where the redox conversion is in the DC regime, E_p becomes independent of the reactant bulk concentration, but is dependent on the scan rate according to the following expression:

$$E_p = E_s + \frac{RT}{nF} \ln\left\{\beta^{1/2}\left(\frac{RTD_R}{nF\nu}\right)^{1/2} \frac{c_S^b}{K_{aR}\Gamma_S^{max}(1-\theta_{O,p})}\right\} \quad (2)$$

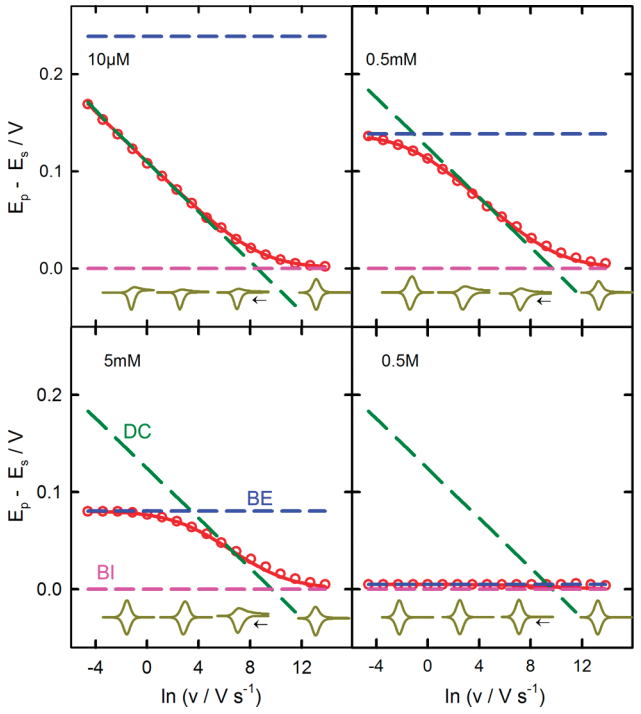

Figure 3. Dependence of the cathodic peak potential on the logarithm of the scan rate for the indicated values of the reactant bulk concentration. Symbols represent the values obtained from simulated cathodic stripping voltammograms for reaction 1, whereas lines represent the predictions of eq 2 (green dashed lines, DC regime), eq 3 (pink dashed lines, BI regime), eq 5 (blue dashed lines, BE regime) and eq 6 (red solid lines). Parameter values: $K_{aR} = 500$, $D_R = 8 \times 10^{-6}$ cm^2 s^{-1}, $c_S^b = 55.5$ M, $r_0 = 0.05$ cm, $\Gamma_R^{max} = \Gamma_O^{max} = \Gamma_S^{max} = 8 \times 10^{-10}$ mol cm^{-2}, $T = 298$ K, and $t_d = 1$ s. Insets (from left to right) represent theoretical voltammetric waveshapes normalized with respect to the cathodic peak current ($i/i_{p,c}$ vs E) for scan rates of 0.1, 10, 10^3, and 10^6 V s^{-1}.

which is valid for linear diffusion and where $\beta = 1.25$, Γ_S^{max} is the surface concentration of a monolayer of clusters of solvent

dx.doi.org/10.1021/ac202564w | *Anal. Chem.* 2012, 84, 1034–1041

molecules of the same size as that for the redox couple, the factor $K_{a,R}\Gamma_S^{max}/c_S^b$ represents a Henry-type adsorption equilibrium constant, and $\theta_{O,p}$ represents the surface coverage of the oxidized redox form at the peak potential ($\theta_{O,p} = \Gamma_{O,p}/\Gamma_O^{max}$), which can be approximated by $\theta_{O,p} \approx 1 - 0.45\theta_{O,ini}$, where $\theta_{O,ini}$ represents the surface coverage at the beginning of the reductive desorption wave. On the other hand, for sufficiently high scan rates, the surface redox conversion enters the BI regime, where E_p becomes independent of the scan rate and is given by

$$E_p = E_s \tag{3}$$

Green and pink dashed lines in Figures 2 and 3 illustrate the predictions of eqs 2 and 3, and how their range of applicability varies with scan rate and reactant concentration.

We have found that the following combination of eqs 2 and 3,

$$E_p = E_s + \frac{RT}{nF}\ln\left\{1 + \beta^{1/2}\left(\frac{RTD_R}{nFv}\right)^{1/2}\frac{c_S^b}{K_{a,R}\Gamma_S^{max}(1-\theta_{O,p})}\right\} \tag{4}$$

is able to reproduce the transition between the DC and BI regimes, so that it can be taken as the general expression for the combined DC + BI regimes.

At high reactant bulk concentrations, where the adsorbed film is equilibrated with the bulk of the solution (BE regime), peak potentials are independent of scan rate, but become dependent on reactant bulk concentration (Figures 2 and 3). This dependence takes the form of (i) a linear variation of E_p with $\ln c_R^b$, whenever the reactant adsorption is small (i.e., when $K_{aR}c_R^b/c_S^b < 0.1$), and (ii) a nonlinear asymptotic approach of E_p to E_s, whenever reactant adsorption is significant (i.e., when $K_{aR}c_R^b/c_S^b > 0.1$). A rigorous analytical expression for the peak potential in the BE regime has been derived previously by White et al.,[23,24] which in our present notation, takes the following form:

$$E_p = E_s + \frac{RT}{nF}\ln\left\{\frac{1 + K_{aR}\left(c_R^b/c_S^b\right)}{K_{aR}\left(c_R^b/c_S^b\right)}\right\} \tag{5}$$

The blue dashed lines in Figures 2 and 3 illustrate how eq 5 is able to reproduce the cathodic peak potential values of simulated voltammograms quantitatively, from low to progressively higher scan rates, when $c_R^b \geq 0.5$ mM.

A close inspection of Figures 2 and 3 reveals that, at the transition between the DC and BE regimes, which typically involves reactant concentrations in the micromolar to millimolar range, E_p varies nonlinearly with the logarithm of either the scan rate or the reactant bulk concentration. This situation results in overestimates of the E_p values by eqs 4 and 5. In an attempt to reach a general description of the peak potential behavior, we have found that the following combination of eqs 4 and 5,

$$E_p = E_s + \frac{RT}{nF} \times \ln\left\{\frac{1 + K_{aR}\left(\frac{c_R^b}{c_S^b}\right)}{\frac{1}{1 + \beta^{1/2}\left(\frac{RTD_R}{nFv}\right)^{1/2}\left[\frac{c_S^b}{K_{aR}\Gamma_S^{max}(1-\theta_{O,p})}\right]} + K_{aR}\left(\frac{c_R^b}{c_S^b}\right)}\right\} \tag{6}$$

is able to reproduce the simulated E_p values over the entire range of relevant parameters of the system, as it is illustrated with the solid red lines in Figures 2 and 3. Thus, eq 6 can be taken as a general expression for the reductive desorption voltammetric peak potential of an electroactive adsorbate, measured under either the normal or the stripping mode of DSV. Its adaptation to the case of an oxidative desorption requires one only to replace the positive sign of the prelogarithmic factor by a minus sign, $(1 - \theta_{O,p})$ by $(1 - \theta_{R,p})$, K_{aR} by K_{aO}, D_R by D_O, and c_R^b by c_O^b in eqs 2−6. Theoretical predictions (Figures S-1−S-3 in the Supporting Information), together with the corresponding analytical expressions (eqs S-14−S-17 in the Supporting Information) for the peak potential of an oxidative desorption, are described in the Supporting Information.

Surface Voltammetric Peak Potential as a Probe of Adsorption Energetics. An attractive aspect of eqs 2−6 is the possibility of determining the adsorption free energy ΔG_{aR}° of the freely diffusing form of the redox couple R via its relationship with K_{aR} ($\Delta G_{aR}^\circ = -RT \ln K_{aR}$). For this purpose, an estimate of the standard formal potential E_s, and also of the reactant diffusion coefficient D_R in the case of the DC regime, is required. An independent estimate of D_R can be obtained from a fit of the number of adsorbed O molecules as a function of the deposition time,[30,31] which can be straightforwardly determined by integrating the baseline-corrected cathodic voltammetric wave measured for distinct deposition times ($\Gamma_O = (nFAv)^{-1}\int i\,dE$). The estimate of E_s is more problematic, since it requires voltammograms to be recorded under experimental conditions such that peak potentials approach the E_s value. This can be achieved either at sufficiently high reactant concentrations, where the system operates in the nonlinear zone of the BE regime, or at sufficiently high scan rates, where the system operates in the BI regime. When neither of these two regimes can be reached, an independent determination of either E_s or K_{aR} is not feasible. However, even in this latter case, one can still determine group contributions to ΔG_{aR}° from the variation of the peak potential with molecular composition and structure. For this purpose, it is convenient to operate under either the DC regime or in the linear zone of the BE regime, since, in both cases, a linear variation of E_p with $\ln K_{aR}$ (or ΔG_{aR}°) is predicted (Figure 4). Note that when the reduced form of the redox couple is strongly adsorbed, the peak potential coincides with E_s and becomes insensitive to the actual value of K_{aR} (the horizontal asymptote in Figure 4), thus precluding any attempt to determine group contributions to the adsorption free energy.

Assuming that the adsorption free energy of reactant R can be split into a summation of group contributions,

$$\Delta G_{aR}^\circ = \sum_J n_J \Delta G_J^\circ \tag{7}$$

where n_J is the number of times that group J appears in the molecular structure and ΔG_J° its contribution to the adsorption free energy. Bearing in mind that $\Delta G_{aR}^\circ = -RT \ln K_{aR}$, the expression for the peak potential in the linear zone of the BE regime ($K_{aR}c_R^b/c_S^b \ll 1$ in eq 5) can be rewritten as

$$E_p^{con} = E_p + \frac{RT}{nF}\ln\left(\frac{c_R^b}{c_S^b}\right) = E_s + \frac{1}{nF}\sum_J n_J \Delta G_J^\circ \tag{8}$$

where E_p^{con} stands for a bulk concentration-corrected peak potential.

dx.doi.org/10.1021/ac202564w | Anal. Chem. 2012, 84, 1034−1041

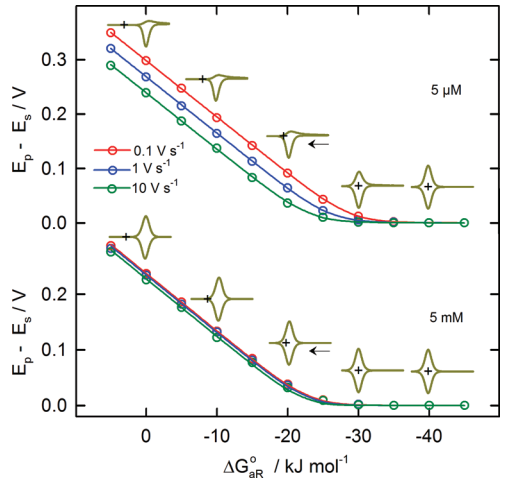

Figure 4. Dependence of the cathodic peak potential on the reactant adsorption free energy for the indicated values of bulk concentration and scan rate. Symbols represent the values obtained from simulated cathodic stripping voltammograms for reaction 1, whereas solid lines represent the predictions of eq 6. Parameter values: $D_R = 8 \times 10^{-6}$ cm^2 s^{-1}, $c_S^b = 55.5$ M, $r_0 = 0.05$ cm, $\Gamma_R^{max} = \Gamma_O^{max} = \Gamma_S^{max} = 8 \times 10^{-10}$ mol cm^{-2}, $T = 298$ K, and $t_d = 1$ s. Insets (from left to right) represent theoretical voltammetric waveshapes normalized with respect to the cathodic peak current ($i/i_{p,c}$ vs E) for $\Delta G^\circ_{aR} = 0$, −10, −20, −30, and −40 kJ mol^{-1}.

The corresponding expression for the peak potential in the DC regime at sufficiently low surface coverages ($1 - \theta_{O,p} \simeq 1$ in eq 2) can be rewritten as

$$E_{p,\theta\approx0}^{dif} = E_{p,\theta\approx0} - \frac{RT}{nF}\ln\left\{\beta^{1/2}\left(\frac{RTD_R}{nFv}\right)^{1/2}\frac{c_S^b}{\Gamma_S^{max}}\right\}$$
$$= E_s + \frac{1}{nF}\sum_J n_J \Delta G_J^\circ \qquad (9)$$

where $E_{p,\theta\approx0}$ stands for the peak potential in the Henry adsorption limit and $E_{p,\theta\approx0}^{dif}$ for its mass-transport-corrected version.

According to eqs 8 and 9, an estimate of the J group contribution to the adsorption free energy (ΔG_J°) can be obtained from the slope of the linear dependence of either E_p^{con} or $E_{p,\theta\approx0}^{dif}$ on n_J. This can be done experimentally by probing the voltammetric features of homologous series of adsorbates that differ in the number of some of their constituent groups. In the next section, we illustrate how eq 9 can be used to determine the contributions of the hydrocarbon groups CH_n ($n = 0$–3) to the adsorption free energy of alkylthiolates on mercury electrodes.

Group Contributions to the Adsorption Free Energy of Alkylthiolates. Oxidatively adsorbed thiols are good candidates to determine the adsorption free energy of individual molecular groups, since they show a simple voltammetric response at low surface coverages,[32] and also because a diversity of closely related molecular structures are readily available. To this end, we have studied the reductive desorption of some carefully chosen homologous series of alkylthiolates, including linear, cyclic, and branched (*iso*- and *tert*-) derivatives. Experimental details are described in the Supporting Information.

To avoid the additional voltammetric features associated with the reductive desorption of standing-up adsorbed thiol molecules that appear for surface coverages exceeding a critical value,[30,33,34] two alternative voltammetric modes have been utilized to assess the effect of the thiolate bulk concentration. Cathodic stripping voltammetry has been the only protocol employed whenever $c_R^b \leq 1$ μM, since the diffusion-controlled deposition is so slow under these circumstances that a preconcentration step is required to adsorb a significant amount of thiol molecules. Then, the additional voltammetric features can be circumvented by adjusting the deposition time to keep the surface coverage below its critical limit.[30,33] Whenever $c_R^b \geq 50$ μM, convenient amounts of thiol are easily deposited, so that an adequate choice of the scan amplitude allows the classical cyclic voltammetry protocol to circumvent the voltammetric features of the standing-up thiol molecules. Finally, the two voltammetric protocols have been used in the intermediate 1−50 μM concentration interval, as proof of their equivalency.

As shown in Figures 5a and 5c for a typical alkanethiol such as *n*-pentanethiol, peak potentials measured with the normal voltammetric mode or the short-time stripping mode in the presence of low thiolate concentrations (<10 μM) are independent of thiol concentration, but are linearly dependent on the logarithm of the scan rate, with a slope (−0.013 V) close to the theoretical value ($-RT/(2nF)$) expected for a monoelectronic reductive desorption operating in the DC regime. On the other hand, E_p values recorded with the cyclic voltammetry mode in the presence of high thiolate concentrations (>0.5 mM) are independent of the scan rate, but vary linearly with the logarithm of thiol concentration as expected for a system operating in the linear zone of the BE regime (blue dashed line in Figure 5a). A similar linear variation has been previously reported by White et al.[23,24] and Uosaki et al.[35] However, a close inspection of the cathodic peak potentials reveals that only for low thiol concentrations and short deposition times (i.e., for low surface coverages), peak potentials follow the trend predicted for the reductive desorption of an homogeneous population of noninteracting monomeric molecules (green solid lines in Figure 5). The observed deviations for high thiol concentrations and/or long deposition times is likely to be due to the presence of dimeric species (such as $Hg(SR)_2$ or $Hg_2(SR)_2$) and/or attractive interactions between the adsorbed molecules.[27,30,36,37] In any of these two cases, the peak potential is expected to follow a unique dependence on the surface concentration, regardless of the voltammetric protocol, the reactant bulk concentration, or the deposition time. As can be judged from Figures 5a and 5b, this is the case for the present system, whenever the thiol surface concentration is below the value corresponding to a standing-up monolayer (i.e., $\ln \Gamma_O < -21.8$) and the thiol bulk concentration is <0.2 mM. Therefore, the concentration dependence of peak potential in the 10 μM < c_R^b < 200 μM interval can be ascribed to the presence of dimers or attractive intermolecular interactions; whereas that observed for higher bulk concentrations can be attributed to the transition from the DC to the BE regime.

Here, we focus on the voltammetric response originated in surface concentration values smaller than ca. 30 pmol cm^{-2}, where adsorbed thiol molecules are lying-down parallel to the electrode surface and both thiol-thiol intermolecular interactions and the presence of dimers can be safely disregarded. For the present experimental conditions, a separate estimate of either E_s or K_{aR} is not possible, since neither the nonlinear zone of the BE regime nor the BI regime are accessible. However, peak potentials measured for low enough thiol coverages and in the presence of low thiol concentrations, i.e., when $E_p \approx E_{p,\theta\approx0}$, can be used to determine group contributions to the adsorption free energy of thiolates through eq 9. To derive $E_{p,\theta\approx0}^{dif}$ values from those of $E_{p,\theta\approx0}$, it is necessary to take into account any

dx.doi.org/10.1021/ac202564w | *Anal. Chem.* 2012, 84, 1034−1041

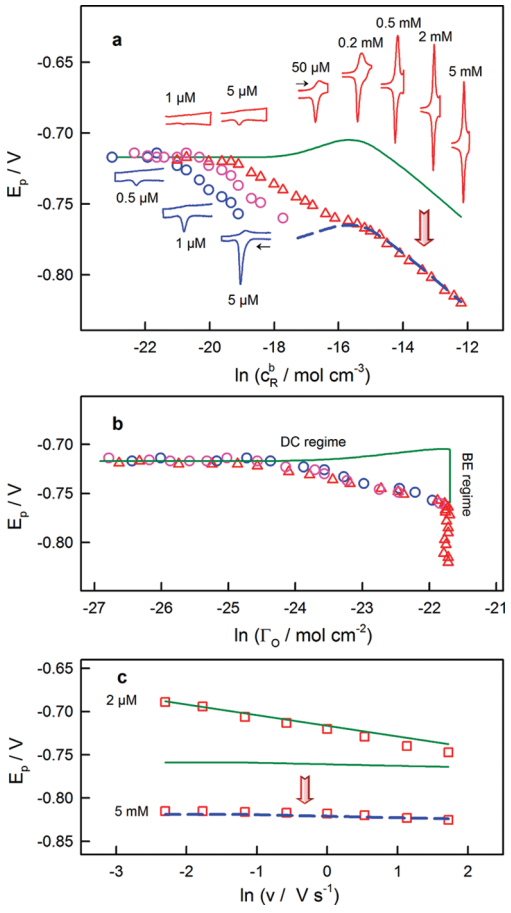

Figure 5. Voltammetric peak potential for the reductive desorption of *n*-pentanethiol as a function of the logarithm of (a) its bulk concentration, (b) its surface concentration, and (c) the scan rate, measured in a solution containing a variable concentration of the thiol and 0.5 M NaOH. Symbols correspond to experimental data obtained by employing either cyclic voltammetry with an anodic forward scan (triangles), or cathodic stripping voltammetry with a deposition time of 10 s (pink circles) or 50 s (blue circles). Green solid lines represent theoretical predictions for a monoelectronic reductive desorption of a homogeneous population of monomeric oxidized adsorbates. Blue dashed lines correspond to an arbitrary shift of the green solid lines along the vertical axis. Insets represent experimental voltammetric wave-shapes obtained with either the cyclic (red) or the cathodic stripping (blue) voltammetric protocol for the indicated *n*-pentanethiol bulk concentrations. Electrode radius = 0.046 cm, scan rate = 1 V s^{-1}, and T = 298 K. The error level of E_p is within ±3 mV (ca. the symbol size).

variation in the diffusion coefficient value of the alkanethiolates under scrutiny. An estimate of D_R has been obtained by fitting surface concentration versus deposition time curves to the solution of the boundary value problem associated with the irreversible thiol adsorption under diffusion control.[30,31] The obtained D_R estimates are randomly distributed between 4.8×10^{-6} and 5.9×10^{-6} cm^2 s^{-1}, which is within the expected error level. Since this dispersion results in a maximum variation of the peak potential of only 3 mV, D_R variations can safely be neglected when comparing peak potentials of different alkanethiolates. Therefore, eq 9 can be reformulated at a given scan rate as

$$E_{p,\theta\approx 0} = B + \frac{1}{nF}\sum_J n_J \Delta G_J^\circ \qquad (10)$$

where B is a constant term.

Figure 6 shows the dependence of $E_{p,\theta\approx 0}$ on the number of carbon atoms n_C of the alkylthiolates of interest. The error level

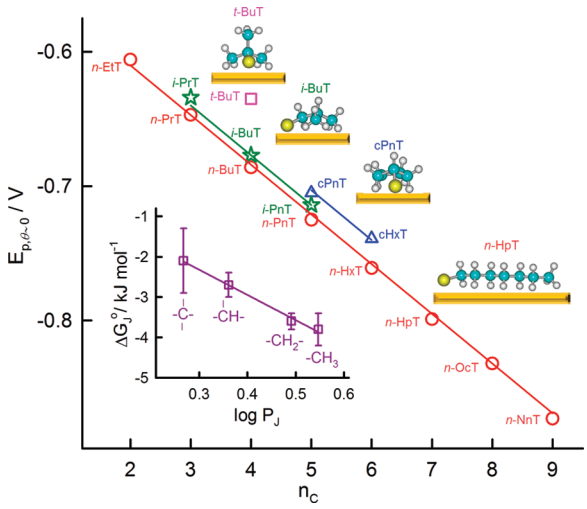

Figure 6. Reductive desorption peak potentials in the Henry adsorption limit for linear (red circles), *iso*- (green stars), *tert*- (pink squares), and cyclic (blue triangles) alkylthiols, measured in a solution containing 2.5 μM thiol and 0.5 M NaOH, as a function of the number of carbon atoms comprising the molecular skeleton. Deposition potential = −0.3 V, surface concentration of deposited thiol molecules = 5 pmol cm^{-2}, scan rate = 1 V s^{-1}, and electrode radius = 0.046 cm. The error level of peak potentials is within ±3 mV (ca. the symbol size). Inset represents the correlation between the contributions of the CH_n (n = 0−3) groups to the adsorption free energy of alkylthiolates at the mercury/solution interface and the logarithm of the octanol−water partition coefficient.[44]

of any $E_{p,\theta\approx 0}$ value has been estimated to be ±3 mV. For each homologous series, a linear variation of $E_{p,\theta\approx 0}$ with n_C has been found, whose slope (−0.037 ± 0.002 V/CH_2) provides an estimate of the methylene group contribution to the thiolate adsorption free energy (eq 10). The obtained $\Delta G^\circ_{CH_2}$ value (−3.6 ± 0.2 kJ mol^{-1}) has been found to be independent of the hydrocarbon structure (linear, cyclic, or branched) and is consistent with that calculated from the results of White et al.[24] for the low-density phase of *n*-alkanethiols adsorbed on mercury. It is also similar to the methylene group contribution to the adsorption free energy of other nonthiolated molecules, such as aliphatic alcohols,[38] acids[39] and esters[40] lying flat at the mercury/solution interface, calculated from the variation of the standard Gibbs energy of adsorption at zero coverage with the number of methylene groups. In all these cases the value of $\Delta G^\circ_{CH_2}$ results from a compromise between the interaction of CH_2 with the underlying substrate and the solvation effects that accompany its adsorption. A rough estimate of these solvation effects can be obtained by comparing our $\Delta G^\circ_{CH_2}$ estimate with that reported by Ocko et al.[41−43] for adsorption at the mercury/air interface (−5.2 ± 0.2 kJ mol^{-1}). This comparison reveals that solvation effects would amount to ca. 1.6 ± 0.3 kJ mol^{-1} per methylene group.

Taking the peak potential of the corresponding linear alkanethiolate as a reference, the following shifts have been found for the desorption peak potential of the iso derivatives (13 mV for *i*-PrT, and 7 mV for *i*-BuT, and *i*-PnT), cyclic alkanethiolates (18 mV), and *tert*-butanethiol (51 mV). The error level for these shifts is within ±4 mV. An estimate of the

dx.doi.org/10.1021/ac202564w | *Anal. Chem.* 2012, 84, 1034−1041

contributions of the CH, CH_3 groups, and of a quaternary carbon atom, to the adsorption energy of alkanethiolates can be obtained by combining these shifts with the difference expressions that result from eq 10, as it is described in the Supporting Information, leading to $\Delta G^{\circ}_{CH} = -2.7 \pm 0.3$ kJ mol^{-1}, $\Delta G^{\circ}_{CH_3} = -3.8 \pm 0.4$ kJ mol^{-1}, and ΔG°_{C}(kJ mol^{-1}) = $-5.9 + 3.8(n^{t\text{-BuT}}_{CH_3,ad} - 1)$, where $n^{t\text{-BuT}}_{CH_3,ad}$ represents the number of methyl groups in the *tert*-butanethiol molecule that are in direct contact with the electrode surface. These estimates point toward a nonlinear increase of $\Delta G^{\circ}_{CH_n}$ with n, when n increases from 1 to 3. However, a close examination of these values indicates that they do vary linearly with the corresponding group contribution to the logarithm of the octanol–water partition coefficient log P_J, which is commonly taken as an hydrophobicity index[44] (see inset in Figure 6). In the case of *tert*-butanethiol, we have found that only $n^{t\text{-BuT}}_{CH_3,ad} = 2$, giving $\Delta G^{\circ}_{C} = -2.1 \pm 0.8$ kJ mol^{-1}, is consistent with the linear ΔG°_{J} vs log P_J correlation found for the CH_n groups. For $n^{t\text{-BuT}}_{CH_3,ad} = 1$ or $n^{t\text{-BuT}}_{CH_3,ad} = 3$, either too negative ($-5.9 \pm 0.7$ kJ mol^{-1}) or too positive (1.7 ± 1.0 kJ mol^{-1}) ΔG°_{C} estimates are obtained. These findings suggest that only two out of the three methyl groups of the *t*-BuT molecule contribute significantly to its adsorption energy. These results stress the high sensitivity of the voltammetric peak potential toward some fine molecular details of the adsorption process.

CONCLUSIONS

A general expression for the surface voltammetric peak potential of an electroactive adsorbate has been derived, taking into account both diffusion and adsorption of the freely diffusing form of the redox couple. Three distinct regimes are distinguished, which correspond to the surface redox conversion being (i) controlled by diffusion (DC regime), (ii) equilibrated with the solution bulk (BE regime), or (ii) isolated from the solution bulk (BI regime). Some strategies to determine group contributions to the adsorption free energy of electroactive adsorbates have been outlined, by taking advantage of the variation of the voltammetric peak potential with molecular composition and structure. These procedures are based on the linear dependence of the voltammetric peak potential on the reactant adsorption free energy, whenever the reactant adsorption is low and its surface redox conversion is either controlled by diffusion or equilibrated with the bulk of the solution. Experimental diagnostic criteria to identify these two regimes have been developed in terms of the dependence of the peak potential on scan rate and reactant bulk concentration. Application to the reductive desorption of distinct homologous series of alkylthiolates has allowed us to determine the contribution of the CH_n (n = 0–3) groups to the adsorption free energy of a large group of alkanethiols. These group contributions have been found to correlate linearly with the octanol–water partition coefficient, suggesting that hydrophobicity drives the adsorption of hydrocarbon groups at the mercury/solution interface.

Overall, this study demonstrates that diffusional surface voltammetry, in either its normal or stripping modes, can be readily used to get quantitative insights into the energetics of electrosorption in the presence of extremely dilute adsorbate solutions (i.e., down to the micromolar level). Given the high sensitivity of the technique, relevant information can be gathered at very low surface coverages, where usual interferences from intermolecular interactions or formation of oligomeric species are absent. From a more general point of view, the present work represents a first step toward the development of a unified treatment of stripping and film voltammetries.

ASSOCIATED CONTENT

Supporting Information

Experimental details, boundary value problem for cathodic diffusional surface voltammetry, surface peak potential for anodic diffusional surface voltammetry, and determination of group contributions to the adsorption free energy of alkanethiolates. This material is available free of charge via the Internet at http://pubs.acs.org.

AUTHOR INFORMATION

Corresponding Author

*Tel.: +34-954557177. Fax: +34-954557174. E-mail: pacheco@us.es.

ACKNOWLEDGMENTS

This work was supported by the Spanish MICINN (under Grant No. CTQ2008-00371) and by the Junta de Andalucia (under Grant No. FQM02492).

REFERENCES

(1) Willner, I.; Katz, E. *Angew. Chem., Int. Ed.* **2000**, *39*, 1180–1218.
(2) Rusling, J. F.; Zhang, Z. In *Biomolecular Films: Design, Function and Applications*; Rusling, J. F., Ed.; Marcel Dekker: New York, 2003; pp 1–64.
(3) Hiemenz, P. C.; Rajagopalan, R. *Principles of Colloid and Surface Chemistry*; Marcel Dekker: New York, 1997.
(4) Carla, M.; Cuomo, M.; Arcangeli, A.; Olivotto, M. *Biophys. J.* **1995**, *68*, 2615–2621.
(5) Baryla, N. E.; Lucy, C. A. *Anal. Chem.* **2000**, *72*, 2280–2284.
(6) Ghosal, S. *Anal. Chem.* **2002**, *74*, 771–775.
(7) Jennings, G. K.; Munro, J. C.; Yong, T.-H.; Laibinis, P. E. *Langmuir* **1998**, *14*, 6130–6139.
(8) Jennings, G. K.; Yong, T.-H.; Munro, J. C.; Laibinis, P. E. *J. Am. Chem. Soc.* **2003**, *125*, 2950–2957.
(9) Bard, A. J.; Faulkner, L. R. *Electrochemical Methods: Fundamentals and Applications*; Wiley: New York, 2001.
(10) Fawcett, W. R. *Liquids, Solutions and Interfaces*; Oxford University Press: New York, 2004.
(11) Wroblowa, H.; Green, M. *Electrochim. Acta* **1963**, *8*, 679–692.
(12) Krauskopf, E. K.; Chan, K.; Wieckowski, A. *J. Phys. Chem.* **1987**, *91*, 2327–2332.
(13) Lipkowski, J.; Stolberg, L.; Morin, S.; Irish, D. E.; Zelenay, P.; Gamboa, M.; Wieckowski, A. *J. Electroanal. Chem.* **1993**, *355*, 147–163.
(14) Barradas, R. G.; Conway, B. E. *J. Electroanal. Chem.* **1963**, *6*, 314–325.
(15) Richer, J.; Lipkowski, J. *J. Electrochem. Soc.* **1986**, *133*, 121–128.
(16) Wandlowski, T.; Hölzle, M. H. *Langmuir* **1996**, *12*, 6597–6603.
(17) Karpovich, D. S.; Blanchard, G. J. *Langmuir* **1994**, *10*, 3315–3322.
(18) Schessler, H. M.; Karpovich, D. S.; Blanchard, G. J. *J. Am. Chem. Soc.* **1996**, *118*, 9645–9651.
(19) Higgins, D. A.; Corn, R. M. *J. Phys. Chem.* **1993**, *97*, 489–493.
(20) Siler, A. R.; Walker, R. A. *J. Phys. Chem. C* **2011**, *115*, 9637–9643.
(21) Powell, H. V.; Schnippering, M.; Mazurenka, M.; Macpherson, J. V.; Mackenzie, S. R.; Unwin, P. R. *Langmuir* **2009**, *25*, 248–255.
(22) Keller, D. W.; Porter, M. D. *Anal. Chem.* **2005**, *77*, 7399–7407.
(23) Hatchett, D. W.; Stevenson, K. J.; Lacy, W. B.; Harris, J. M.; White, H. S. *J. Am. Chem. Soc.* **1997**, *119*, 6596–6606.

(24) Stevenson, K. J.; Mitchell, M.; White, H. S. *J. Phys. Chem. B* **1998**, *102*, 1235−1240.
(25) Hatchett, D. W.; Uibel, R. H.; Stevenson, K. J.; Harris, J. M.; White, H. S. *J. Am. Chem. Soc.* **1998**, *120*, 1062−1069.
(26) Wang, J. *Analytical Electrochemistry*; John Wiley & Sons: New York, 2006.
(27) Calvente, J. J.; Andreu, R.; Gil, M. L. A.; Gonzalez, L.; Alcudia, A.; Dominguez, M. *J. Electroanal. Chem.* **2000**, *482*, 18−31.
(28) Calvente, J. J.; Andreu, R. *Anal. Chem.* **2011**, *83*, 6401−6409.
(29) Calvente, J. J.; Gil, M. L. A.; Andreu, R.; Roldan, E.; Domínguez, M. *Langmuir* **1999**, *15*, 1842−1852.
(30) Calvente, J. J.; Andreu, R.; Gonzalez, L.; Gil, M. L. A.; Mozo, J. D.; Roldan, E. *J. Phys. Chem. B* **2001**, *105*, 5477−5488.
(31) Ramírez, P.; Andreu, R.; Calvente, J. J.; Calzado, C. J.; López-Pérez, G. *J. Electroanal. Chem.* **2005**, *582*, 179−190.
(32) Calvente, J. J.; Andreu, R. *Phys. Chem. Chem. Phys.* **2010**, *12*, 13519−13521.
(33) Calvente, J. J.; López-Pérez, G.; Jurado, J. M.; Andreu, R.; Molero, M.; Roldán, E. *Langmuir* **2010**, *26*, 2914−2923.
(34) Calvente, J. J.; Molero, M.; Andreu, R.; López-Pérez, G. *Langmuir* **2010**, *26*, 5254−5261.
(35) Sumi, T.; Uosaki, K. *J. Phys. Chem. B* **2004**, *108*, 6422−6428.
(36) Stankovich, M. T.; Bard, A. J. *J. Electroanal. Chem.* **1977**, *75*, 487−505.
(37) Gil, M. L. A.; Andreu, R.; Calvente, J. J.; de Pablos, F. *J. Electrochem. Soc.* **2002**, *149*, E45−E54.
(38) Moncelli, M. R.; Foresti, M. L.; Guidelli, R. *J. Electroanal. Chem.* **1990**, *295*, 225−238.
(39) Damaskin, B.; Frumkin, A.; Chizhov, A. *J. Electroanal. Chem.* **1970**, *28*, 93−104.
(40) Damaskin, B. B. *Russ. J. Electrochem.* **2005**, *41*, 355−360.
(41) Kraack, H.; Ocko, B. M.; Pershan, P. S.; Sloutskin, E.; Deutsch, M. *J. Chem. Phys.* **2003**, *119*, 10339−10349.
(42) Kraack, H.; Ocko, B. M.; Pershan, P. S.; Sloutskin, E.; Tamam, L.; Deutsch, M. *Langmuir* **2004**, *20*, 5386−5395.
(43) Kraack, H.; Ocko, B. M.; Pershan, P. S.; Sloutskin, E.; Tamam, L.; Deutsch, M. *Langmuir* **2004**, *20*, 5375−5385.
(44) Meylan, W. M.; Howard, P. H. *Perspect. Drug Discovery Des.* **2000**, *19*, 67−84.